SYNTHESIS, CHARACTERIZATION AND ACUTE AQUATIC TOXICITY OF SAMARIUM OXIDE NANOPARTICLES TO FRESHWATER GREEN ALGAE

KUZNÍKOVÁ Ľubomíra[1], DĚDKOVÁ Kateřina[1,2], KUPKOVÁ Jana[1,2], VÁŇA Rostislav[3], KUKUTSCHOVÁ Jana[1,2]

[1]*Nanotechnology Centre, VSB - Technical University of Ostrava, Czech Republic, EU*
lubomira.kuznikova@vsb.cz

[2]*Regional Materials Science and Technology Centre, VSB - Technical University of Ostrava, Czech Republic, EU*

[3]*TESCAN Brno, s.r.o., Brno, Czech Republic, EU*

Abstract

The article describes the preparation of samarium oxide nanoparticles (nano Sm_2O_3) via thermal decomposition of a transient complex formed *in situ* from $Sm(NO_3)_3 \cdot 6H_2O$ and glycine and its acute aquatic toxicity to *Chlorella vulgaris*. The resulting nanoparticles were characterized by X-ray powder diffraction analysis, which showed the Sm_2O_3 nanoparticles to be with the crystallite size of 11 nm. Morphology of the Sm_2O_3 nanoparticles was examined by scanning and transmission electron microscopy. Electron diffraction observed in transmission electron microscopy corresponds to the results obtained from X-ray diffraction analysis. The elemental composition of the product was confirmed by EDS analysis. Freshwater green algae (*C. vulgaris*) served as a model organism for evaluation of acute aquatic toxicity. Effective concentration of toxicity EC_{50} was determined for the concentration of 2.43 gr.l^{-1},of Sm_2O_3 nanoparticles in the fresh water green algae strain.

Keywords: Thermal decomposition, acute aquatic toxicity, algae *Chlorella vulgaris*, samarium oxide nanoparticles (nano Sm_2O_3)

1. INTRODUCTION

Lanthanide oxides have gained a lot of attention due to their diverse use for applications such as in the optical materials, nuclear industry, lasers, and electronics [1]. One of the significant rare earth oxides is Sm_2O_3, due to its physical properties, such as wide band gap (4.33 eV) and high refractive index (1.93) [2]. Sm_2O_3 nanoparticles are thermally stable and are used in semiconductors, solar cells, infrared absorbing glass, catalysts, and in biological and of gas sensors [3,4].

Currently, the increasing production and usage of Sm_2O_3 nanoparticles for various industrial applications raised questions and concerns about their impact on human health and environment [5]. To date, relatively low amount of information has been gained on bio-accumulation and its influence on animals, plants, human health and the environment in general. Available literature dealing with these influences is mostly limited to samarium nitrate [6,7], samarium chloride [8,9] and samarium oxide in bulk form (particle size of about 5 μm) [10].

Consequently, the aim of the work was preparation and characterization of Sm_2O_3 nanoparticles and evaluation its acute aquatic toxicity to freshwater green algae *Chlorella vulgaris*.

2. EXPERIMENTAL

2.1. Synthesis of samarium oxide nanoparticles

Demineralized water from the column Demiwa 10 (Watek) was used for the preparation of solutions. Samarium nitrate ($Sm(NO_3)_3 \cdot 6H_2O$) was purchased from Sigma Aldrich company (Germany) in reagent grade quality and glycine (NH_2CH_2COOH) was purchased from Lachner (Czech Republic) in p. a. quality.

Samarium oxide nanoparticles (nano Sm_2O_3) were prepared by the thermal decomposition of the complex formed by the salt $Sm(NO_3)_3 \cdot 6H_2O$ and glycine (NH_2CH_2COOH). The reaction protocol was used as in previous studies [11, 12]. The following scheme illustrates synthesis of Sm_2O_3 nanoparticles:

$$Sm(NO_3)_3 \cdot 6\,H_2O\,(s) + NH_2CH_2COOH\,(s) \xrightarrow[-\,N_2\,(g),\,CO_2\,(g),\,H_2O\,(g)]{600\ ^\circ C,\ 1\ hour} Sm_2O_3\,(s)\,. \quad (1)$$

The yield of the chemical reaction was determined to an average value of 55.43 % (0.45 g).

2.2. Characterization of samarium oxide nanoparticles

X-ray powder diffraction analysis was performed using the X-ray diffractometer Ultima IV Rigaku (Rigaku, Japan), operated at 40 kV and 40 mA with CuKα radiation (reflection mode, Bragg-Brentano arrangement, scintillation counter). The XRD patterns were recorded in the 10 - 70° 2θ range with a scanning rate of 2 °/min. The samples were placed in a ground glass depression in the sample holder and flattened with a glass slide. X-ray beam was demarcated by 2/3° divergence, 10 mm divergent height limiting, 2/3° scattering, and 0.6 mm receiving slits. Phase analysis was evaluated by database PDF-2 Release 2011. Graphic processing of XRD pattern was made using OriginPro8. The Sm_2O_3 reflection of the (222) plane was used to determine crystallite size using the Scherrer formula [13]

$$L_{222} = \frac{K \cdot \lambda}{\beta \cdot \cos\theta}\,, \quad (2)$$

where K (K = 0.94) is the factor of microstructure, β is the full-width at half-maximum (FWHM), λ is the wavelength of radiation, and θ is the diffraction angle.

Scanning electron microscope MAIA3 (TESCAN) - ultra-high resolution SEM with Schottky field emission cathode - was used for electron micrographs and EDS analysis. Images were taken by using a combination of InBeam SE and Low-Energy BSE detector at 1.7 kV. EDS analysis was performed with X-MaxN 150 (Oxford instruments) and the EDS data were processed in AZtec software. Furthermore, the product morphology was also observed by scanning electron microscope Quanta 450 FEG (FEI). Images were taken by SE detector at 15 kV.

Product morphology and electron diffraction was also observed by transmission electron microscope JEOL1200EX at 120 kV. Powder sample was stirred in distilled water and an appropriate specimen amount was placed on copper grid with carbon film.

2.3. Acute aquatic toxicity bioassay

Acute aquatic toxicity test was done according to the ČSN EN ISO 8692 Standard [16] and OECD Guideline 201 [15]. The aim of the test was to determine the median inhibition concentration EC_{50}, i.e. the concentration of a toxicant which causes 50 % inhibition of algal cells growth in comparison with control [16]. As detection organism for the evaluation of toxicity, *Chlorella vulgaris* (Institute of Botany of the Academy of Sciences of the Czech Republic in Třeboň), freshwater green algae, was used.

Toxicity tests were conducted with 3 days old algae culture. Before the test, number of cells was counted using light microscope Olympus CX31 (Olympus) and Bürker chamber and the added volume of culture at the beginning of the toxicity test to the suspension of nutrient medium and nanoparticles of Sm_2O_3 was calculated. In the beginning toxicity tests suspension of Sm_2O_3 nanoparticles with concentration 2.5 $g \cdot l^{-1}$ were prepared. The prepared suspension was diluted to the selected concentrations: 2.5 $g \cdot l^{-1}$, 2.0 $g \cdot l^{-1}$, 1.5 $g \cdot l^{-1}$, 1.0 $g \cdot l^{-1}$, 0.5 $g \cdot l^{-1}$. Due to the validity of the tests, two parallel tests were carried out at the same time. When the pH of the tested samples did not match within the physiological range (8.3 ± 0.2), it was adjusted with 1 $mol \cdot l^{-1}$ solutions of sodium hydroxide (NaOH) or hydrochloric acid (HCl). The samples prepared for the toxicity tests were placed in the conditioned box APT.line™ KBW (E5.1) with temperature (23 ± 2) °C, with 24 hours

exposure to daylight on a horizontal shaker KS 260 Basic (IKA) with (125 ± 25) rpm. Toxicity tests were performed over a period of (72 ± 2) hours. At the end of the test, the cells were counted using light microscope and Bürker chamber and growth inhibition (EC_{50}) from the number of cells was determined.

3. RESULTING AND DISCUSSION

3.1. Characterization of the prepared sample

The thermal decomposition of the complex produced light white product. The XRD pattern in **Figure 1A** shows the single phase of Sm_2O_3 (PDF card No. 01-086-2479) with cubic crystal structure. The crystallite size of reflection (222) plane was about 11 nm. The results from XRD correspond to the results electron diffraction (**Figure 1B**) observed in transmission electron microscope.

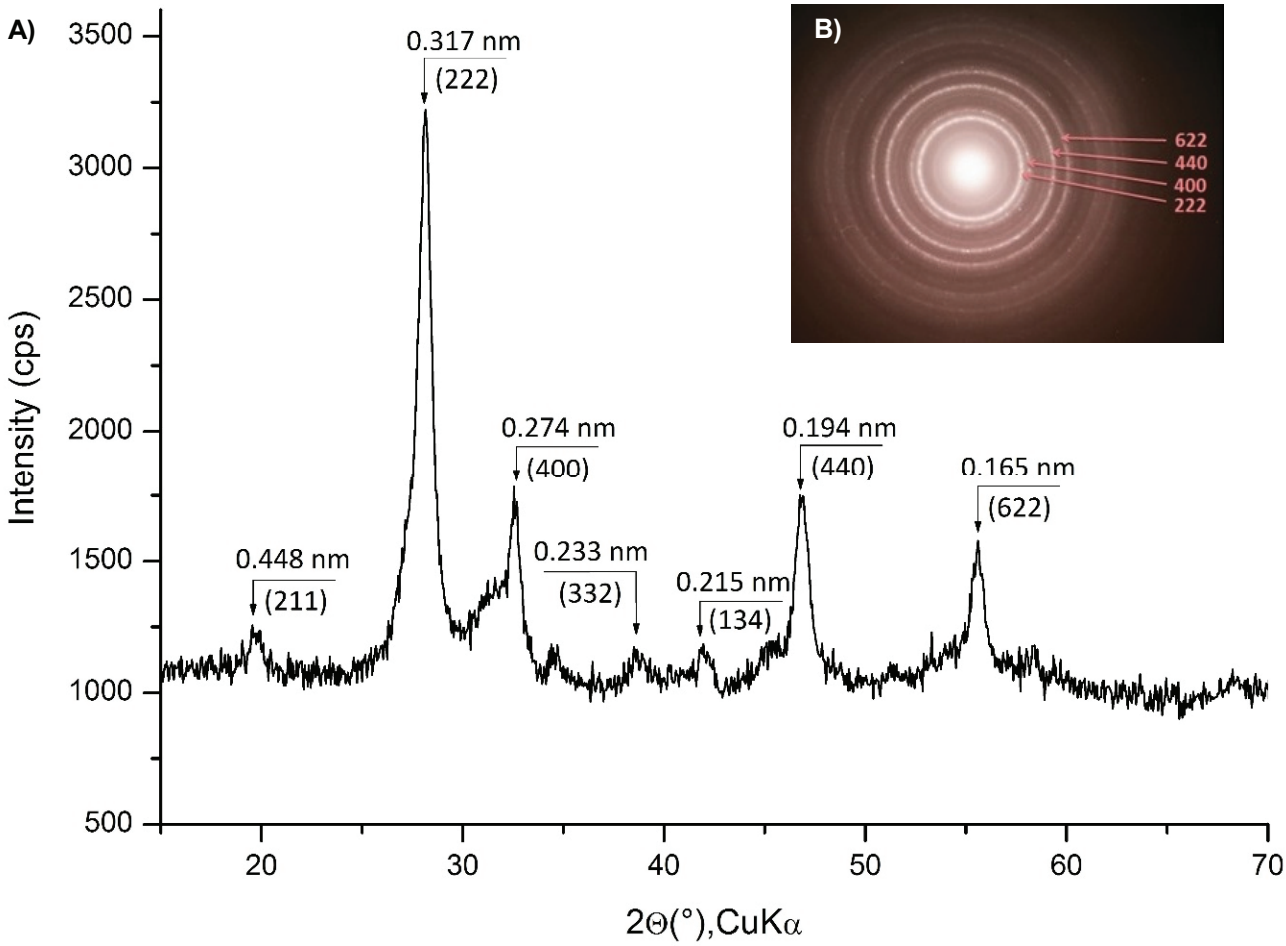

Figure 1 X-ray powder diffraction pattern **(A)** and electron diffraction patterns **(B)** of the prepared nanoparticles

EDS (**Figure 2A**) confirmed the presence of samarium and oxygen in the prepared sample. From the SEM images (**Figure 2B**) it can be seen that Sm_2O_3 nanoparticles, due to influence of the electrostatic forces, organize aggregates. The network configuration of sample can be observed at the lower magnification. At the higher magnification, it can be seen that the sample appears as porous mousse with meso- and macro-pores. The structure of the sample is strongly influenced by the reaction mechanisms however detailed description and explanation of this phenomenon is under current investigation.

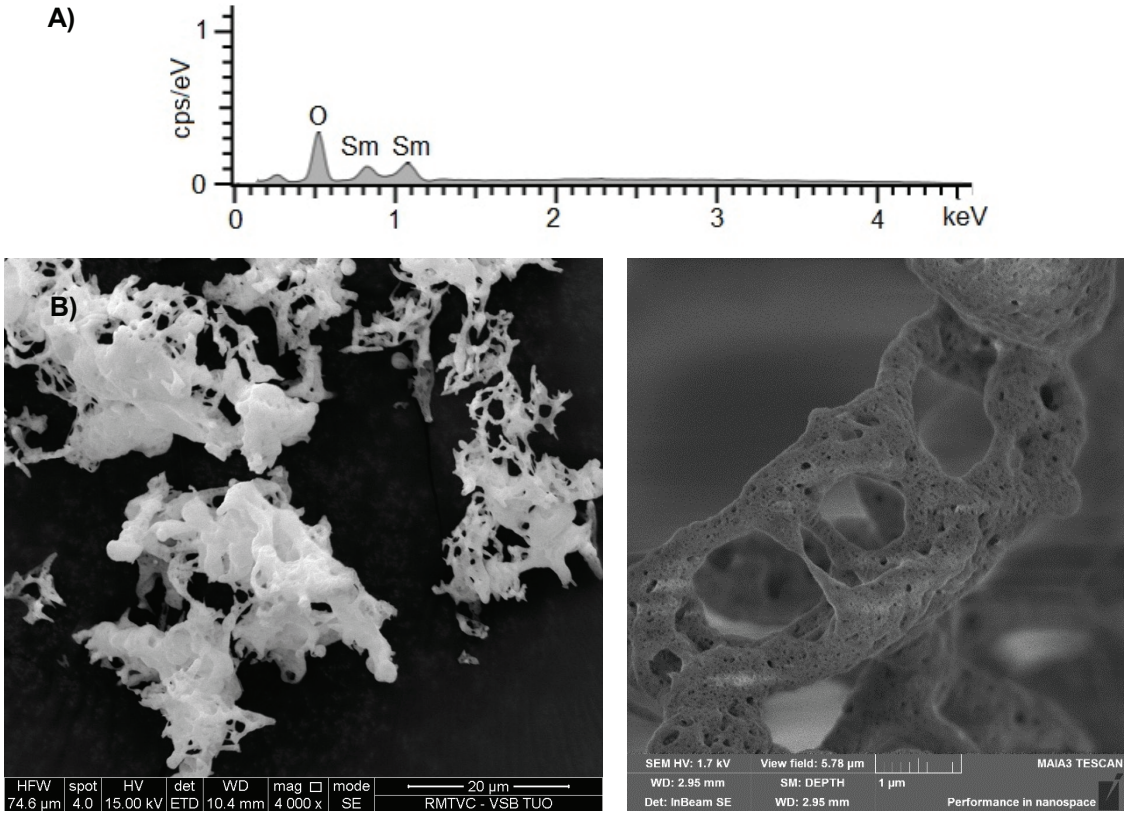

Figure 2 EDS spectrum of the sample **(A)** and SEM images of the sample at different magnifications **(B)**

From the bright field TEM image (**Figure 3A**) aggregates with net-like morphology of the sample can be observed. The dark field TEM image (**Figure 3B**) show crystals which aggregate. Further, the results from TEM are consistent with the results from scanning electron microscopy.

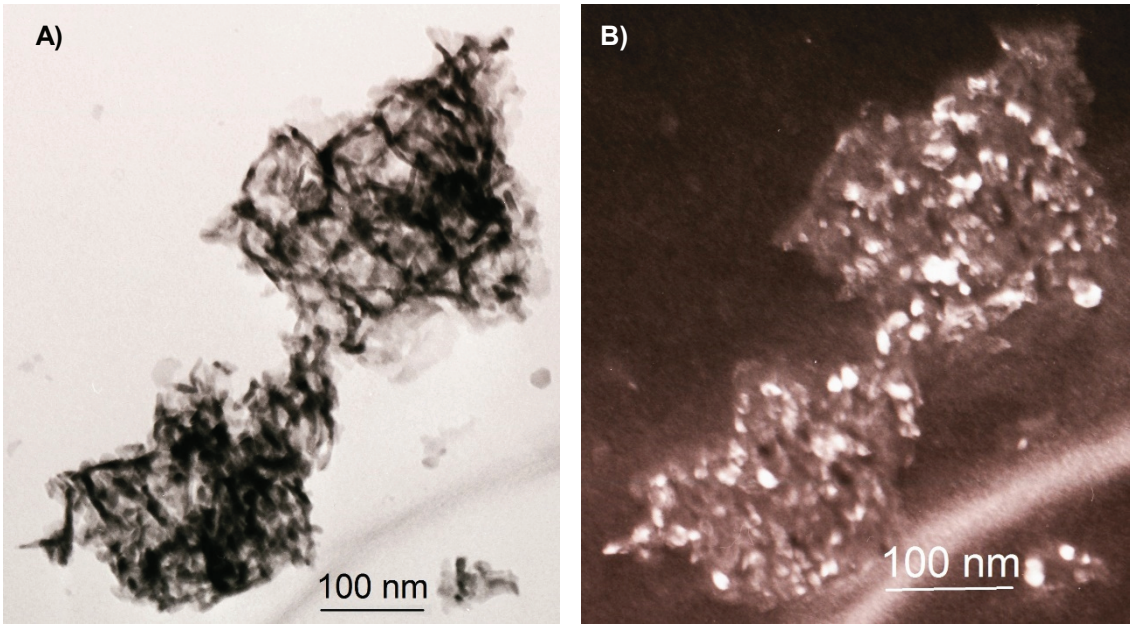

Figure 3 TEM images of the sample at bright field **(A)** and dark field **(B)**

3.2. Acute aquatic toxicity

Toxicity tests were evaluated after exposure of (72 ± 2) hours. Effective concentration of toxicity (EC_{50}) was determined from the acquired experimental data (**Table 1**). EC_{50} was subtracted from the biomass growth curve inhibition in % to a concentration of the sample in $g \cdot l^{-1}$ (**Figure 4**). The parameter EC_{50} was determined for the concentration 2.43 $g \cdot l^{-1}$ of Sm_2O_3 nanoparticles to freshwater green algae *C. vulgaris.*

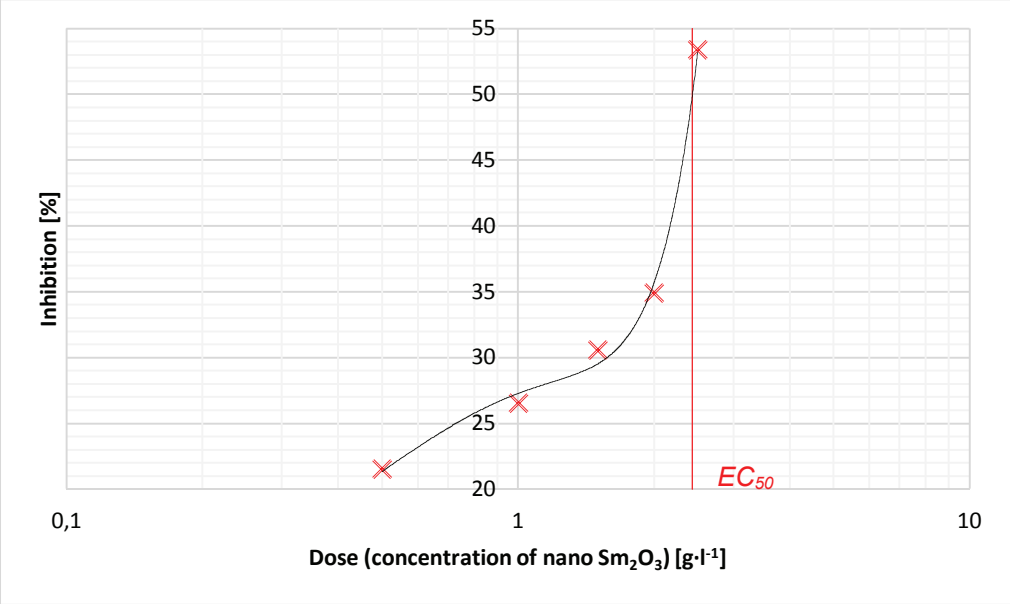

Figure 4 Biomass growth inhibition curve of Sm_2O_3 nanoparticles

Table 1 The values of biomass growth inhibition for the selected concentrations of Sm_2O_3 nanoparticles

Dose (concentration of nano Sm_2O_3) [$g \cdot l^{-1}$]	Inhibition [%]
2.5	53.38
2.0	34.91
1.5	30.59
1.0	26.55
0.5	21.54

4. CONCLUSION

Sm_2O_3 nanoparticles with crystallinity size of 11 nm were prepared by the thermal decomposition of the complex created by $Sm(NO_3)_3 \cdot 6H_2O$ and glycine. Consequently, acute aquatic toxicity to freshwater green algae (*C. vulgaris*) of the prepared Sm_2O_3 nanoparticles was evaluated for acute aquatic toxicity to freshwater green algae (*C. vulgaris*). It was found that 50 % inhibition of algal growth in culture is caused by the concentration of 2.43 $g \cdot l^{-1}$ of Sm_2O_3.

The increase of toxicological studies of compounds and nanomaterials containing samarium is evident, however there is heterogeneity in the used methods and obtained results. Especially there is a lack of information about the toxicity of Sm_2O_3 nanoparticles to freshwater green algae. Toxicity of Sm_2O_3 nanoparticle on algal cultures *Desmodesmus subspicatus* and *Raphidocelis subcapitata* was described in our previous work

[11]. Where EC_{50} was determined equal to 1.73 $g \cdot l^{-1}$ for *Desmodesmus sp.* and 0.65 $g \cdot l^{-1}$ for *Raphidocelis sp.* from a comparison of EC_{50} factors is clear that, freshwater green algae *C. vulgaris* is the least sensitive to Sm_2O_3 nanoparticles than *Desmodesmus sp.* and *Raphidocelis sp*.

It is evident that an inseparable part of the evaluation of the toxicity of nanomaterials is the characterization of their physicochemical properties, because this knowledge is important for comparability between studies. Hereinafter, for the future it is important to evaluate of toxicity to other detection organisms, because each organism reacts differently to the same toxicant. Finally, it is important to establish proper methodology for evaluation of the toxicity of nanomaterials, which are not currently sufficient in comparison with conventional methods to assess the toxicity of other materials.

ACKNOWLEDGEMENTS

This study was funded by projects Reg.No. SP2017/75 and LO1203 "Regional Materials Science and Technology Center - Feasibility Program" (Ministry of Education, Youth and Sports of the Czech Republic). The authors declare that they have no conflict of interest.

REFERENCES

[1] TSUZUKI, T., PIRAULT, E., MCCORMICK, P. Mechanochemical synthesis of gadolinium oxide nanoparticles. *Nanostructured Materials.* 1999, vol. 11, no. 1, pp. 125-131.

[2] RENGANATHAN, B., SASTIKUMAR, D., SRINIVASAN, R., GANESAN, A. Nanocrystalline samarium oxide coated fiber optic gas sensor. *Materials Science and Engineering: B*. 2014, vol. 186, pp. 122-127.

[3] MUNEER, I., FARRUKH, M., JAVAID, S., SHAHID, M., KHALEEQ-UR-RAHMAN, M. Synthesis of Gd_2O_3/Sm_2O_3 nanocomposite via sonication and hydrothermal methods and its optical properties. *Superlattices and Microstructures.* 2015, vol. 77, pp. 256-266.

[4] MOHAMMADINASAB, R., TABATABAEE, M., AGHAIE, H., SEYED SADJADI, M. A Simple Method for Synthesis of Nanocrystalline Sm_2O_3 Powder by Thermal Decomposition of Samarium Nitrate. *Synthesis and Reactivity in Inorganic, Metal-Organic, and Nano-Metal Chemistry.* 2014, vol. 45, no. 3, pp. 451-454.

[5] DOMÍNGUEZ, A., ARISTIMUÑO, C., ARRIAGA, E., ASPIAZU, A., SUÁREZ-MERINO, B., GOÑI-DE-CERIO, F. Acute and subchronic pulmonary toxicity of cerium oxide nanoparticles for safety assessment. *Toxicology Letters*. 2013, vol. 221, pp 239.

[6] ZHANG, D. -Y., SHEN, X.-Y., RUAN, Q., XU, X.-L., YANG, S.-P., LU, Y., XU, H.-Y., HAO, F.-L. Effects of subchronic samarium exposure on the histopathological structure and apoptosis regulation in mouse testis. *Environmental Toxicology and Pharmacology*. 2014, vol. 37, no. 2, pp. 505-512.

[7] WEILIN, S., XIUYING, S., XIYING, M. Effects of Samarium on Liver and Kidney of Rats. *Journal of Rare Earths*. 2006, vol. 24, no. 1, pp. 415-418.

[8] TAI, P., ZHAO, Q., SU, D., LI, P., STAGNITTI, F. Biological toxicity of lanthanide elements on algae. *Chemosphere.* 2010, vol. 80, no. 9, pp.1031-1035.

[9] PAGANO, G., GUIDA, M., SICILIANO, A., et al. Comparative toxicities of selected rare earth elements: Sea urchin embryogenesis and fertilization damage with redox and cytogenetic effects. *Environmental Research*. 2016, vol. 147, pp. 453-460.

[10] SHINOHARA, A., MATSUKAWA, T., CHIBA, M., KUMASAKA, T., KOBAYASHI, J., TAKAMORI, K., ICHINOSE, S., YOKOYAMA, K. Comparative study of behavior of inhaled samarium and cerium in mice. *Journal of Rare Earths.* 2010, vol. 28, pp. 507-509.

[11] DĚDKOVÁ, K., KUZNÍKOVÁ, Ľ., PAVELEK, L., et al. Daylight induced antibacterial activity of gadolinium oxide, samarium oxide and erbium oxide nanoparticles and their aquatic toxicity. *Materials Chemistry and Physics.* 2017, vol. 197, pp. 226-235.

[12] KUZNÍKOVÁ, Ľ., DĚDKOVÁ, K., PAVELEK, L., KUPKOVÁ, J., VÁŇA, R., KUKUTSCHOVÁ, J. Synthesis and Characterization of Samarium Oxide Nanocrystallites. *Journal of Nanoscience and Nanotechnology*. 2016, vol. 16, no. 8, pp. 7829-7831.

[13] SCHERRER, P. Estimation of the previous and internal structure of colloidal particles by means of roentgen rays. Nach Ges Wiss Gottingen. 1918, p. 96-100.

[14] ČESKÁ TECHNICKÁ NORMA ISO 8692. *Kvalita vod - Zkouška inhibice růstu sladkovodních zelených řas*. 2004. Český normalizační institut, 2005.

[15] *OECD guidelines for testing chemicals: Alga, Growth Inhibition Test.* Organization for economic cooperation and development, 1984, no. 201.

[16] CHEN, Z., BERTIN, R., FROLDI, G. EC_{50} estimation of antioxidant activity in DPPH assay using several statistical programs. *Food Chemistry*. 2013, vol. 138, no. 1, pp. 414-420.